



**HAL**  
open science

# Generalizing the Hand Redirection Function in Virtual Reality

Benoît Geslain, Simon Besga, Flavien Lebrun, Gilles Bailly

► **To cite this version:**

Benoît Geslain, Simon Besga, Flavien Lebrun, Gilles Bailly. Generalizing the Hand Redirection Function in Virtual Reality. AVI 2022 - International Conference on Advanced Visual Interfaces, Jun 2022, Rome, Italy. pp.#33, 10.1145/3531073.3531100 . hal-03699315

**HAL Id: hal-03699315**

**<https://hal.sorbonne-universite.fr/hal-03699315v1>**

Submitted on 20 Jun 2022

**HAL** is a multi-disciplinary open access archive for the deposit and dissemination of scientific research documents, whether they are published or not. The documents may come from teaching and research institutions in France or abroad, or from public or private research centers.

L'archive ouverte pluridisciplinaire **HAL**, est destinée au dépôt et à la diffusion de documents scientifiques de niveau recherche, publiés ou non, émanant des établissements d'enseignement et de recherche français ou étrangers, des laboratoires publics ou privés.

# Generalizing the Hand Redirection Function in Virtual Reality

Benoît Geslain\*

Sorbonne University, CNRS, ISIR  
SEGULA Technologies  
France

Flavien Lebrun

Sorbonne University, CNRS, ISIR  
France

Simon Besga\*

Sorbonne University, CNRS, ISIR  
LIRMM, University of Montpellier, CNRS  
France

Gilles Bailly

Sorbonne University, CNRS, ISIR  
France

## ABSTRACT

Hand redirection is a visuo-haptic illusion offering rich haptic feedback in Virtual Reality while using a limited number of physical objects. This technique relies on a redirection function which determines the virtual hand position depending on the physical hand position. In this paper, we extend the design space of the Hand-redirection technique by generalizing this redirection function. A user study compares 6 redirection functions. Our results suggest that the redirection function does not deteriorate the illusion offering more flexibility and control to designer over the hand trajectory and avoid collisions.

## CCS CONCEPTS

• **Human-centered computing** → **HCI theory, concepts and models**; *Pointing*.

## KEYWORDS

Virtual Reality, Haptic Feedback, Visuo-haptic Illusion, Hand Redirection

## 1 INTRODUCTION

Visuo-haptic illusions exploit visual dominance to enrich user immersion in virtual reality (VR). For example, users can interact with many virtual objects despite a limited number of props (physical objects) present in the physical environment [14, 22]. It is also possible to modify an object shape [1, 8] or its physical properties like weight [9, 20, 30] or stiffness [25]. When a conflict arises between sight and another sense (typically proprioception), our brain solves it by placing more trust in sight [5, 15]. **Hand redirection** [2, 6] is one of these visuo-haptic illusions. This technique creates a mismatch between users' real and virtual hand on purpose. When users reach for an object, their virtual hand is offsetted from their real hand to match both real and virtual hands with the matching target. When the user touches the real object, it provides a haptic confirmation. This made-up sensory consistency between sight and touch makes it credible [18, 31]. When the mismatch between the two hand is too large, the illusion is detected by users and the immersion is deteriorated [28].

Previous work extensively studied the influence of the distance between the virtual and the physical target on the detection of the illusion [35], but not the behavior of the virtual hand. The **redirection function** creates this behavior by determining the position of the virtual hand depending on the position of the physical hand. While there is theoretically an infinite number of redirection functions, previous studies rely on the same one.

In this paper, we study the design space of redirection function on their influence on the (non-) detection of the illusion. In addition to the linear (degree=1) redirection function used in previous works, we consider second-degree polynomial functions. This gives us better control of the offset between the virtual and physical hand and ultimately of the hand trajectory when reaching the target.

We then carry out a user study. We compare 6 new redirection functions to the one used in the literature. The results show that these new redirection functions do not deteriorate the illusion while offering more flexibility to designers. Indeed, our results suggest that designers can manipulate the trajectory of the real hand and thus avoid potential collisions with physical objects or even with robots [16, 23].

## 2 RELATED WORK

We first discuss the visuo-haptic illusions, on which the *Hand Redirection* technique is based. We then describe precisely how hand redirection is implemented and evaluated in the literature.

### 2.1 Visuo-haptic Illusions

Visuo-haptic illusions manipulate a user's perception of their body and/or environment by creating a conflict between their sight and proprioception. These illusions are used to enhance realism, interaction space and/or multimodal feedback in VR [1, 8]. They are mainly based on visual dominance [15, 18]. When sight conflicts with a sense (in this case proprioception), it tends to be privileged to resolve the conflict [10, 11]. Several virtual reality interaction techniques exploit this visual dominance. For example, by reducing or increasing the translations and rotations of the user's head, one can imperceptibly manipulate the sensation of walking in a straight line [29, 32, 33]. It is also possible to manipulate the visual representation of virtual objects or the user's avatar, for example, to alter the perception of the weight of an object [9, 20, 30], its size [4] or the stiffness of a spring [25].

\*These authors contributed equally.

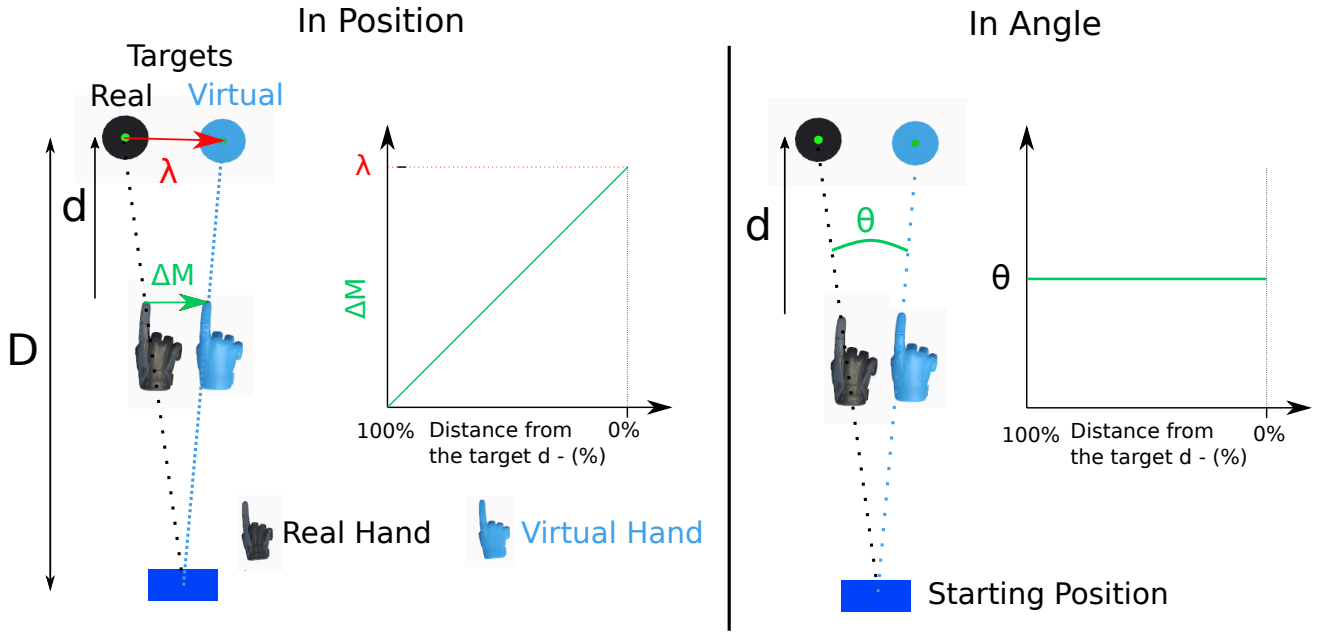


**Figure 1: Common hand redirection techniques in VR.** On the left, the virtual hand’s position (blue) is computed by adding a portion of vector  $\vec{\lambda}$  to it according to the distance  $d$ . On the right, the virtual hand’s position is computed by rotating the real hand’s position around the starting position by the angle created by the targets. Both descriptions are equivalent.

## 2.2 Hand Redirection

Hand redirection is a particular visuo-haptic illusion where the avatar of the user’s hand (virtual hand) is progressively displaced from the real hand during a movement [21]. Both hands (real and virtual ones) are no longer co-located which creates a specific mapping between a real and virtual surface or object. When this offset is not detected, the user relies on information from their vision (i.e. the position of their virtual hand) to estimate the position of their real hand. One of the main applications of this illusion is to use a single physical object as a proxy for several virtual objects [7, 19, 26]. For instance, a user can interact with three virtual cubes. However, there is only one physical cube needed in the real environment. During movement towards one of the virtual cubes, the user’s virtual hand is redirected so that the real hand always reaches the real cube [2]. This illusion can also be a tool for two-handed interaction [26] or active interface enhancement [1]. In the following section, we detail the implementation of this technique.

## 2.3 Usual Implementation

A common implementation of the hand redirection illusion is the *Interpolated Reach* [19]. They define the offset between the real hand and the virtual hand  $\vec{\Delta}_M$  with a linear function of the distance between the **Real Hand**  $\vec{P}_H^R$  and the **Real Target**  $\vec{P}_T^R$ . The position of the **Virtual Hand** is then equation 1.

$$\vec{P}_V^H = \vec{P}_R^H + \vec{\Delta}_M(\vec{P}_H^R, \vec{P}_T^R) \quad (1)$$

$$\vec{\Delta}_M(\vec{P}_H^R, \vec{P}_T^R) = \left(1 - \frac{\|\vec{P}_H^R - \vec{P}_T^R\|}{\|\vec{P}_O - \vec{P}_T^R\|}\right) \vec{\lambda} \quad (2)$$

with  $P_O$  the starting point which defines the area where the illusion is activated and  $\lambda = \|\vec{P}_T^V - \vec{P}_T^R\|$  the vector formed by the real and virtual targets. For ease of reading, we define the distance between the real hand and the target  $d = \|\vec{P}_H^R - \vec{P}_T^R\|$  and the distance between the starting point and the real target  $D = \|\vec{P}_O - \vec{P}_T^R\|$ . Thus, equation ?? becomes

$$\vec{\Delta}_M(d) = \left(1 - \frac{d}{D}\right) \vec{\lambda} \quad (3)$$

Note that  $D$  and  $\vec{\lambda}$  are constant and as the real hand reaches the target, only  $d$  fluctuates. This equation is then a simple linear equation with two parameters  $\{-\frac{\lambda}{D}, \vec{\lambda}\}$ . Equation 3 guarantees that when the real hand is on the starting position ( $d = D$ ), the offset  $\vec{\Delta}_M$  is null and when the real hand reaches the real target ( $d = 0$ ),

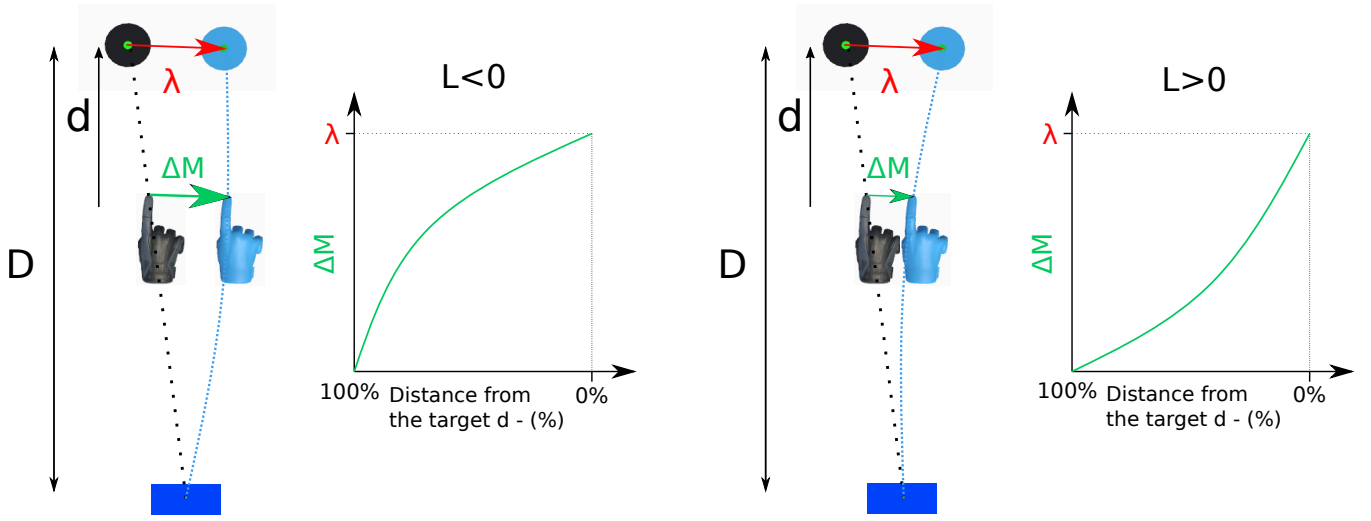


**Figure 2: The hand redirection technique with a  $2^{nd}$  order polynomial function. On the left, the function ( $L < 0$ ) redirects the user faster at the start of the movement rather than at the end. Inversly, on the right, the function ( $L > 0$ ) redirects the user faster at the end of the movement rather than at the start. The offset curves ( $\Delta_M$ ) are the same than those figure 8.**

the offset equals  $\vec{\lambda}$ . In the case where the hand is further from the real target ( $d > D$ ), the offset is set to 0. This implementation can be seen on the left panel of figure 1. In an other implementation, the virtual hand position is set by rotating the virtual hand around the starting position using the angle formed by the real target, the starting position and the virtual target [24, 35]. This implementation can be seen on the right panel of figure 1. Both implementations are equivalent.

## 2.4 Detection Threshold

We evaluate and compare these techniques by estimating when a user detects an illusion: the maximum offset between the real and virtual targets for example. Typically, we determine when an illusion is correctly detected 75% of the time by varying a single illusion parameter like the redirection angle [35] (see figure 1-right). The parameter value found is called the detection threshold.

Different experimental protocols have been used to determine the detection threshold. The most common is the 2 Alternative Forced Choice (2AFC) [3, 12, 17, 24, 27, 35]: for each trial, the participant is exposed to the illusion for a given parameter value. At the end of the trial, the participant is asked to indicate in which direction their virtual hand is compared to their real hand. Hence, the participants make a binary choice (left or right). When repeated enough times it allows to determine the probability of detection of the illusion for each illusion parameter studied.

In summary, many implementations of hand redirection have been proposed and most of them rely on a linear redirection function. In this article, we generalize the equation 3 by considering polynomial functions of order greater than 1 (order 2). We then analyze the influence of these functions on the illusion detection threshold.

## 3 GENERALIZATION OF THE HAND REDIRECTION FUNCTION

Equation 3 is a first order polynomial:  $f_1(d) = (a \times d + b)$ . We generalize this equation:

$$\vec{\Delta}_M(d) = \begin{cases} f_n(d)\vec{\lambda} & \text{if } d < D \\ 0 & \text{otherwise} \end{cases} \quad (4)$$

with  $f_n(d)$  a polynomial of degree  $n$  with two constraints:  $f_n(D) = 0$  and  $f_n(0) = 1$ . These polynomials allow to create a large variety of redirection behaviour like redirecting faster at the start or the end of the movement. The polynomial function is then

$$f_n(d) = \sum_{i=0}^n (a_i d^i) \quad (5)$$

with  $a_i$  the  $i^{th}$  coefficient to be determined. When  $n = 1$  (see equation 3), there is no degree of freedom, we have  $a_1 = -\frac{1}{D}$  and  $a_0 = 1$  because of the continuity constraints at the target and the starting position. With  $n > 1$ , the function has 1 or more degrees of freedom.

In this article, we focus on second-order polynomials and their influence on the detection threshold of the hand redirection illusion. In this case, equation 4 becomes

$$\vec{\Delta}_M(d) = f_2(d)\vec{\lambda} = (a_2 d^2 + a_1 d + a_0)\vec{\lambda} \quad (6)$$

This equation has 1 degree of freedom because there are only 2 constraints for 3 parameters. Figure 2 shows two examples satisfying the constraints. We chose to write the equation with a Bézier Curve [13] to represent the degrees of freedom with control points that can easily be manipulated visually.

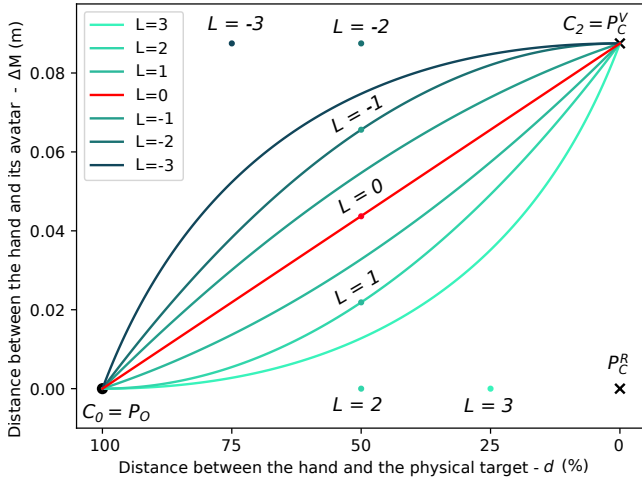


**Figure 3: The offset between the real and its avatar  $\Delta_M$  according to the distance between the real hand and the physical target  $d$ . The red curve is the standard linear redirection function  $L = 0$ ; the six additional curves are the second-degree polynomial functions. Above the red curve  $L < 0$ , the redirection is applied faster at the beginning of the movement. Below the red curve  $L > 0$ , the redirection is applied faster at the end of the movement. In this case, the redirection is applied for an offset  $\Delta_M$  of 8.75cm or 5°.**

A Bézier Curve defines a polynomial of degree  $n$  from  $n + 1$  control points ( $P_{C_i}$ ):

$$B(\vec{t}) = \sum_{i=0}^n \binom{n}{i} (1-t)^{n-i} t^i \vec{P}_{C_i} \quad (7)$$

with  $n$  the order of the polynomial,  $B_x(t) = D - d$  and  $B_y(t) = \|\vec{\Delta}_M\|$  and  $t$  the Bézier variable varying between 0 and 1. The first ( $P_{C_0}$ ) and last ( $P_{C_n}$ ) control points correspond respectively to the starting position and the virtual target position. The other control points allow to visually control the speed at which the redirection is applied as the user approaches the target.<sup>1</sup>

In this formalism, equation 3 is a Bézier curve with two control points  $\vec{P}_{C_0} = (D, 0)$  et  $\vec{P}_{C_1} = (0, 1)$ . For a second-order polynomial, equation 7 becomes

$$B(\vec{t}) = (1-t)^2 \vec{P}_{C_0} + 2t(1-t) \vec{P}_{C_1} + t^2 \vec{P}_{C_2} \quad (8)$$

where  $P_{C_1}$  is the control point representing our degree of freedom. Figure 3 illustrates 6 redirection functions by varying the position of the control point  $P_{C_1}$ . We define each redirection function with a variable  $L$ . For  $L < 0$ , the virtual hand is redirected away from the real hand faster than with the linear function.

And the opposite is true for  $L > 0$ . Finally, for all functions, the virtual and real hands are at the same position when the real hand is at the starting point and offset by  $\|\vec{\lambda}\|$  when the real hand is at the targets.

<sup>1</sup>In reality, because our input variable is  $d$  and not  $t$ , it is necessary to solve this two equation system by determining  $t$  according to  $d$  and then computing the offset  $B_y(t)$ .

## 4 USER STUDY

The aim of this user study is to evaluate the influence of non-linear redirection functions on the detection threshold of the hand redirection illusion. We focus on second-order polynomials illustrated in figure 3. The experimental protocol is similar to Lebrun et al. [24] and Zenner et al. [35] where participants realize a pointing task in VR. After each repetition, participants select a Two Alternative Forced Choice (2AFC) about the direction of redirection (Left or Right) as well as if they detected the illusion (Yes or No).

### 4.1 Participants and Apparatus

The study was conducted with 19 participants (9 male, 10 female), aged from 20 to 29 years old (23.8 average). All participants were students volunteer from Sorbonne University. Amongst them, 2 were left-handed, 1 ambidextrous, and 15 right-handed. All participants had normal or corrected to normal eyesight (5 participants wore glasses or contact lenses). 3 of them had a regular VR experience, 11 had previous VR experience and 3 had no experience at all. No participants had musculoskeletal or proprioception disorders.

This user experiment was approved by the ethics comity of Sorbonne Université n°2020-020.

Participants were seated in front of a table wearing a VR HMD (HTC VIVE Pro) and a hand harness with a VIVE Tracker attached to it (see Figure 4). The position and orientation of the hand and finger are tracked with a precision of 1mm and 0.3°. We choose the HTC VIVE Pro because it was available and provide an appreciable confort for the participants. However our experiment protocol could be reproduced with a more accessible VR HMD.

A blue haptic marker is placed on the table as a starting position. 4 targets are arranged in an arc of a circle 56cm away from the starting point and offset by 15° from each other. We choose this distance so that all participants could reach the targets while seated. Similarly, the angular offset is set greater than the largest angle offset and small enough that participants couldn't detect it. Targets have a push-button on top for the users to press. Targets on the far right and far left are dummies and participants never interact with them. They are here to further "hide" the illusion from participants seeing the real setup before putting the HMD on.

The virtual scene illustrated in figure 4 is a copy of the real environment. It was created in the Unity3D editor. The hand is represented with a static hand with the index pointing forward. During a trial, only a single virtual target is shown to the user, the one they should point at.

### 4.2 Experimental Design

**4.2.1 Task and Stimulus.** The experiment is a pointing task with a Two Alternative Forced Choice (2AFC) similar to Zenner et al.'s experiment [35] which is the most common protocol for studying these illusions and allows to compare our results. The task starts with the user's finger on the starting position, a virtual target then appears. The participant reaches the target, presses the physical button, and goes back to the starting position. We ask that participants move naturally and avoid sudden movements and do the entire movement in 4 seconds. Then, participants have to choose if they had detected the illusion or not and if their real hand was on

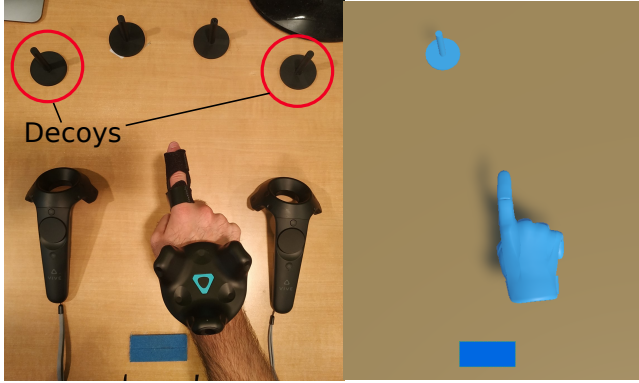


**Figure 4:** On the left, the table with 4 targets (including 2 decoys), the haptic marker and a participant’s hand with the VIVE tracker. On the right, what the user sees: a single target, the hand avatar and the haptic marker.

the left or on the right of their virtual hand. This first question is an extension of the more typical protocol. In cases where participants make a mistake with the largest amplitude of redirection ( $14^\circ$  et  $-14^\circ$ ), the ground becomes red to notify them. From preliminary results and the state of the art [3, 35], participants should always be able to correctly guess the redirection direction in this case. No further information were given to participants.

**4.2.2 Conditions.** We control 3 independant variables. The first variable is the FUNCTION OF REDIRECTION  $L$  with 7 values:  $L = -3, -2, -1, 0, 1, 2, 3$  (see figure 3). Note that  $L = 0$  is the linear reference function [19, 35].

The second variable is the REDIRECTION AMPLITUDE  $\theta$ . It is the angle formed by the real target, the starting position, and the virtual target. We consider 9 values:  $-14^\circ, -10^\circ, -6^\circ, -2^\circ, 0^\circ, 2^\circ, 6^\circ, 10^\circ, 14^\circ$ . The extreme values should be easily detectable ( $14^\circ$  and to some extent,  $10^\circ$ ) whereas the closest values to  $0^\circ$  should be very hard to detect ( $2^\circ$ ). We compromised between having values covering a large enough spectrum to have easily detectable values, enough points to fit a psychometric curve on our data, and restricting the experiment time per participant (<1h).

The last variable is the PHYSICAL TARGET, Left or Right Target, introducing variability in the user’s gesture. The leftmost and rightmost physical targets are not used in the experiment.

**4.2.3 Procedure.** Participants are first informed about the objective of the study and the task they need to perform. Careful attention was brought on explaining the concept of hand redirection and how to correctly answer the 2AFC: "Your virtual hand is represented in the virtual scene. During the task, an offset is added gradually between this virtual hand and your real hand. This offset shifts the virtual hand either on the left or on the right of your real hand." Participants then put the hand harness and the HMD on. Participants had time to accommodate with the illusion and the virtual scene by doing 4 training trials where their real hand was visible on top of their shifted virtual hand. The offset values were

$-10^\circ, -2^\circ, 2^\circ$  et  $10^\circ$ . After each trial, participants were informed of the direction of redirection. They then realize the full experiment without seeing their real hand position. At the end, they fill out a demographic questionnaire.

**4.2.4 Design.** This study follows a within-subject design. Each participant did 2 repetitions of each combination of the 9 REDIRECTION AMPLITUDES, 7 REDIRECTION FUNCTIONS and 2 PHYSICAL TARGETS, i.e. 2 blocks of 126 trials. The different conditions are pseudo-randomized in each bloc. In summary, the experimental design is  $18 \text{ Participants} \times 2 \text{ blocks} \times 9 \text{ REDIRECTION AMPLITUDES} \times 7 \text{ REDIRECTION FUNCTIONS} \times 2 \text{ PHYSICAL TARGETS} = 4284$  repetitions.

## 5 ANALYSIS

A typical analysis of this kind of experiment (2AFC) consists in plotting the psychometric curve of the population to estimate the detection threshold of the illusion.

### 5.1 Psychometric Curve

A psychometric curve (figure 6) consists in plotting the probability of answering one choice of the 2AFC over a controlled parameter. The resulting curve can be fitted with a sigmoid:

$$P(X) = \frac{1}{1 + e^{-\frac{X-a}{b}}} \quad (9)$$

where  $a$  and  $b$  are two parameters used to adjust the fit.  $X$  is the controlled parameter and  $P(X)$  is the probability to answer one of the two force choices. In our case, it’s the probability that the participant chose Left over the REDIRECTION AMPLITUDE  $P(X = \theta)$ . Intuitively,  $P(\theta)$  closes in on 100% when the virtual hand is indeed on the left of the real hand in higher amplitudes and inversely, closes in on 0% when the virtual hand is on the right of the real hand.

### 5.2 Point of Subjective Equality

The point of Subjective Equality  $PSE$  is where participants perceive the real gesture as equal to the virtual one. Graphically, it is where the curve crosses the 50% probability. Essentially, participants answer randomly to the 2AFC. It is expected that this value is close to a REDIRECTION AMPLITUDE of  $0^\circ$ .

### 5.3 Detection Threshold and Interval of Non-Detection

The psychometric curve allows to determine detection thresholds by looking for  $\theta$  so that  $P(\theta = IND_G) = 25\%$  and  $P(\theta = IND_D) = 75\%$  [25, 35].  $IND_G$  is the detection threshold when the virtual hand is redirected on the left of the real hand and vice-versa for  $IND_D$ . We use the reciprocal function of equation 9:

$$X = -b \ln \left( \frac{1}{P(IND)} - 1 \right) + a \quad (10)$$

The Interval of Non-Detection ( $IND$ ) is then  $IND = IND_D - IND_G$ . It represents the span of REDIRECTION AMPLITUDE where participants don’t detect the hand redirection illusion.

The main aim of our analysis is to estimate if and how the  $IND$  is influenced by the REDIRECTION FUNCTION.



## 6 RESULTS

### 6.1 Outliers

We removed participants from the analysis when any of the following conditions were met:

- The left or right non-detection interval  $IND$  for the linear redirection function ( $L = 0$ ) is less than  $-14^\circ$  or greater than  $14^\circ$ , similar to [3].
- The correct response percentage is less than 80% for the  $14^\circ$  and  $-14^\circ$  angles and for the linear redirection function ( $L = 0$ ).

Therefore, 3 participants were excluded for a detection interval of  $15.0^\circ$ ,  $16.2^\circ$  and  $28.5^\circ$  and one participant for a correct response rate of 60%. The results presented here are therefore those of the 15 remaining participants. The experimental design is therefore : 15 Participants  $\times$  2 blocks  $\times$  9 REDIRECTION AMPLITUDE  $\times$  7 REDIRECTION FUNCTIONS  $\times$  2 PHYSICAL TARGETS = 4032 repetitions.

### 6.2 Target effect

We calculated the non-detection interval ( $IND$ ) for each of the two physical targets and each redirection function . A Two-Way ANOVA (PHYSICAL TARGETS  $\times$  REDIRECTION FUNCTIONS) on  $IND$  indicates no significant effect of PHYSICAL TARGETS ( $F_{1,15} = 0.003, p > 0.05$ ), nor interaction effects ( $F_{6,15} = 0.984, p > 0.05$ ).

### 6.3 Redirection Function effect on Detection

A One-Way ANOVA (REDIRECTION FUNCTION) for each REDIRECTION AMPLITUDE on the illusion detection question shows no significant effect on the detection.

### 6.4 Interval of Non-Detection

Figure 6 shows psychometric curve for each REDIRECTION FUNCTION. The vertical bars indicate the Left and Right Intervals of Non-Detection. They vary on the left from  $-7.75^\circ$  to  $-3.45^\circ$  and on the right from  $3.99^\circ$  to  $6.79^\circ$ . Non-detection interval in the linear case  $L = 0$  is  $IND = 10.6^\circ$ .

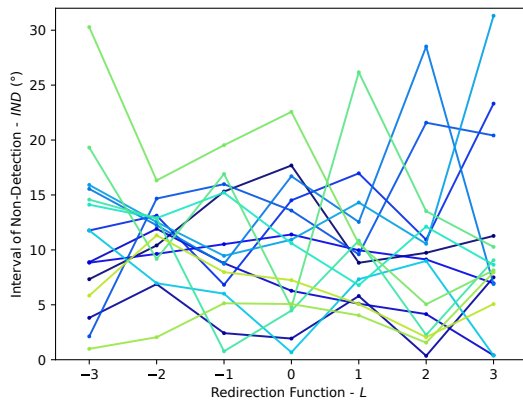


Figure 5: The interval of non-detection  $IND$  for each redirection function and for each participant.

These values are comparable to the results of Zenner *et al.* in [35]. The distance between the source and the target is within the same magnitude and their results are very close with a  $IND = 8.19^\circ$ . The results reported by [27] and [3] show higher  $IND$  (respectively  $IND = 26.7^\circ$  and  $IND = 44.6^\circ$ ). However, the distance between the origin and the real target is much smaller: around  $20cm$  for the first one, and variable value for the second one (around  $24cm \pm 7, 5cm$ ), against  $56cm$  in our study.

Figure 7 represents Intervals of Non-Detection according to the redirection functions  $L$ . The area around the curve represents the 95% confidence interval calculated with the 1000-sample Bootstrap technique. The curve tends to be constant, which would indicate that the detection interval appears to be invariant to the redirection function. A One-Way ANOVA of the REDIRECTION FUNCTION over the  $IND$  reveals no significant difference:  $F_{8,15} = 0.876, p > 0.05$ . An equivalence test carried out on all pairs of  $L$  REDIRECTION FUNCTION, the Two One-sided T-test (TOST), confirms the equivalence with the lower limit  $-3.5^\circ$  and the upper limit  $+3.5^\circ$  ( $p < 0.05$ ). Nevertheless, the TOST does not allow us to conclude on the equivalence of the  $IND$  with  $-2^\circ$  and  $+2^\circ$  bounds.

We therefore did not find any significant effect of the REDIRECTION FUNCTION on the detection of the illusion.

### 6.5 Point of Subjective Equality

Figure 7 shows the  $PSE$  for the different redirection functions. For the linear case  $L = 0$ , the  $PSE$  is  $-0.23^\circ$ . As for  $IND$ , our value of  $PSE$  is similar to the results obtained by Zenner *et al.* [35], with a  $PSE = -0.28^\circ$ .

A Two-Way ANOVA (PHYSICAL TARGETS  $\times$  REDIRECTION FUNCTION) on the  $PSE$  indicates no significant effect of PHYSICAL TARGETS ( $F_{1,15} = 3.491, p > 0.05$ ) nor interaction effect ( $F_{6,15} = 1.895, p > 0.05$ ).

Table 1 shows a summary of our results.

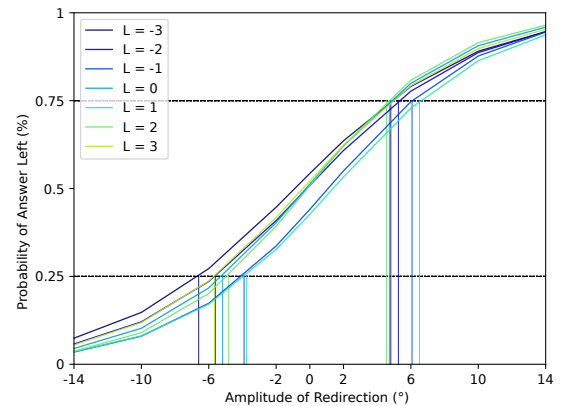
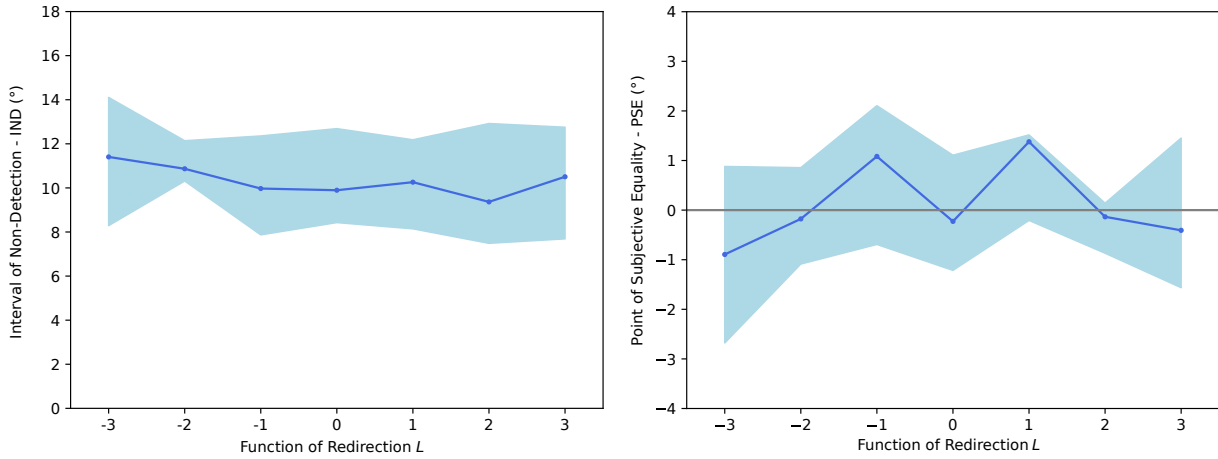


Figure 6: The psychometric function for each redirection function according to the angle of redirection. Vertical lines show the interval of non-detection  $IND$  for a redirection on the right (25%) and on the left (75%).



**Figure 7: On the left, the interval of non-detection  $IND$  according to the redirection function. On the right, the point of subjective equality  $PSE$  according to the redirection function. The colored area shows the 95% confidence intervals computed with the bootstrap method.**

## 6.6 Participant Analysis

Figure 5 shows the non-detection interval for each user (one colour per participant) depending on the redirection function. We do not observe any particular pattern such as groups of behaviors.

## 7 HAND TRAJECTORY ANALYSIS

We logged the positions of the hand over time to analyse the real hand trajectory when reaching for the target as a function of the redirection function. We first removed trajectories where the hand tracking was not optimal (<5%) and then grouped trajectories for all participants by amplitude of redirection and redirection function.

Figure 8 illustrate all the trajectories as a function of the function of redirection for the redirection amplitude  $14^\circ$ . We observe that the trajectory shape is influenced by the redirection function  $L$ : a strong redirection at the beginning of the movement ( $L < 0$ ) generates a smooth reversed  $C$  shaped trajectory (Figure 8-Left). In contrast, a strong redirection at the end of the movement ( $L > 0$ ) generates a trajectory with a stronger correction at the end of the movement. (Figure 8-Right).

	IND	PSE
$L=-3$	$11.41^\circ$	$-0.89^\circ$
$L=-2$	$10.87^\circ$	$-0.18^\circ$
$L=-1$	$9.97^\circ$	$1.08^\circ$
$L=0$	$9.89^\circ$	$-0.23^\circ$
$L=0$ [35]	$8.19^\circ$	$-0.28^\circ$
$L=1$	$10.26^\circ$	$1.38^\circ$
$L=2$	$9.37^\circ$	$-0.13^\circ$
$L=3$	$10.51^\circ$	$-0.41^\circ$

**Table 1: Summary of our results: Interval of Non-Detection  $IND$  and Point of Subjective Equality  $PSE$  as a function of the function of redirection  $L$ . Results in [35] are given for comparison purpose.**

## 8 DISCUSSION

This paper explores the design space of redirection functions for the hand redirection technique: we generalized the current implementation by considering polynomials of degree 2. The main objective of the user study was then to investigate the influence of the redirection functions on the interval of non-detection of the illusion. We considered 6 redirection functions with different dynamics (a shift at the beginning or at the end of the movement). Our results show no significant effect of the redirection function on the interval of non detection. Moreover, a Two-One Sided T-test (TOST) suggests the equivalence of the non-detection intervals for the different redirection functions.

We now discuss possible explanations why different redirection functions do not affect the detection of the illusion. A two-component model suggests that an aimed movement is divided into two phases: first a ballistic movement followed by a correction movement [34]. In the ballistic phase, the movement is faster as the users do not rely on vision to correct errors. Recent studies [2, 14] about visuo-haptic illusions show that some participants strongly adjust their trajectory of their real hand towards the target only during the final part of the movement. This observation is in line with the two-component model suggesting that participants only noticed the offset between the predicted and actual position of the virtual hand at the end of the ballistic movement.

By generalising the redirection functions, we can choose whether the offset between the real and the virtual hand mainly increases during the ballistic phase or the correction phase. Indeed, with  $L < 0$ , the offset is likely to increase during the ballistic phase (beginning of the movement) while while  $L > 0$ , the offset is likely to increase during the correction phase (end of the movement). A difference regarding the detection of the illusion between  $L < 0$  and  $L > 0$  would suggest that users are more sensitive to the offset increase in one of the two phases. In particular, we thought that the amplitude of the offset at the end of the ballistic phase would influence the detection of the illusion.



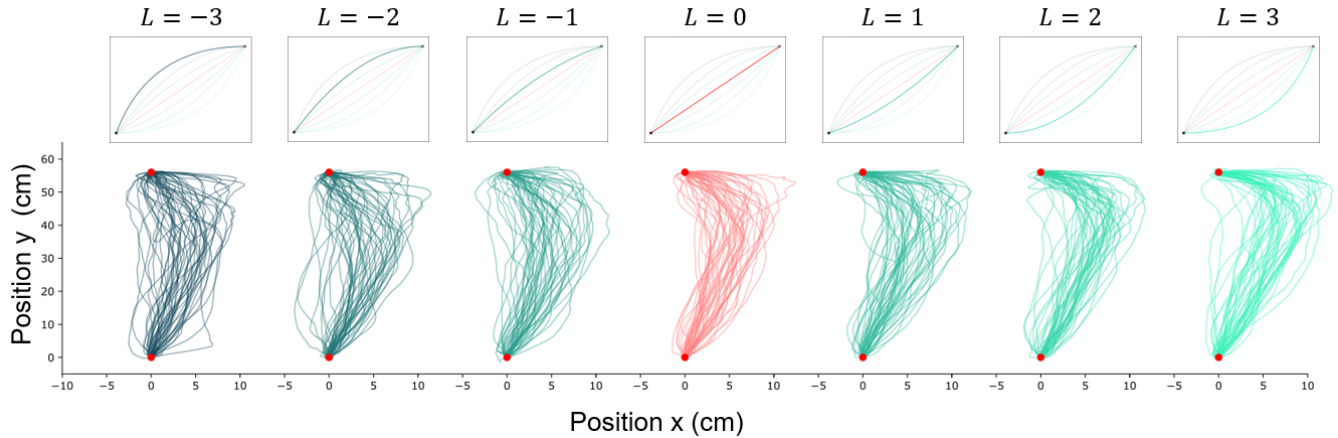


**Figure 8: A visualization of participants trajectories for each redirection function evaluated. These trajectories come from all trials with a redirection amplitude of  $14^\circ$  on both physical targets.**

Surprisingly, our results do not show differences regardless of the value of  $L$ . One explanation could be that users are not sensitive to when the offset increases, but only to the maximum offset amplitude at the end of the trial, i.e. when the users touch the physical target. Another explanation might be that the ballistic phase is much shorter than expected. Participants' movements could have been too slow due to our instructions favoring correction movements. Participants could also have focused too much on their virtual hand, rather than the target to accurately answer the 2AFC choice. As future work, we plan to study possible interaction effects between movement speed and redirection function. Indeed, faster movements and potentially more contrasted redirection functions could make some phenomena more salient. Future work should also control the effect of the distance from the real hand to the body as the visual and proprioceptive accuracy might vary in the ballistic (currently close to the body) and correction phase (far from the body). For instance, we will consider a reverse movement where the starting position of the hand is away from the body and the target is close to the body. Another possible explanation is that an effect is present but not visible due to the lack of data points. Future work should consider a larger number of participants and/or a larger number of samples per participant. The instructions might have been more difficult to interpret than expected as some participants might have noticed the visuo-haptic mismatch but were not able to correctly indicate the direction of the mismatch.

## 9 IMPLICATIONS FOR DESIGN

Our results have implications for design interactions. They suggest the designer can better control the real hand trajectory during the hand redirection. For example, in a complex scene with multiple physical objects that can be accidentally hit, the designer can use an appropriate function to avoid any obstacles along the real hand's path. Also, many interaction techniques revolve around using actuated robots to provide haptic feedback. It is conceivable to alter the hand's trajectory to avoid unwanted contact with the robot.

## 10 CONCLUSION

In this article, we generalized the redirection function of the hand redirection techniques by considering other redirection functions like  $2^{nd}$  order polynomials. We empirically compared the influence of 6 of those functions with the standard linear function. Our results suggest that the redirection function does not influence the Interval of Non-Detection. We also found that the redirection function offers more flexibility to designers to control the hand trajectory.

## ACKNOWLEDGMENTS

We would like to thank the participants of this study.

## REFERENCES

- [1] Parastoo Abtahi and Sean Follmer. 2018. Visuo-Haptic Illusions for Improving the Perceived Performance of Shape Displays. In *Proceedings of the 2018 CHI Conference on Human Factors in Computing Systems* (Montreal QC, Canada) (CHI '18). ACM, New York, NY, USA, Article 150, 13 pages. <https://doi.org/10.1145/3173574.3173724>
- [2] Mahdi Azmandian, Mark Hancock, Hrvoje Benko, Eyal Ofek, and Andrew D. Wilson. 2016. Haptic Retargeting: Dynamic Repurposing of Passive Haptics for Enhanced Virtual Reality Experiences. In *Proceedings of the 2016 CHI Conference on Human Factors in Computing Systems* (San Jose, California, USA) (CHI '16). ACM, New York, NY, USA, 1968–1979. <https://doi.org/10.1145/2858036.2858226>
- [3] Brett Benda, Shaghayegh Esmaeili, and Eric D. Ragan. 2020. Determining Detection Thresholds for Fixed Positional Offsets for Virtual Hand Remapping in Virtual Reality. In *2020 IEEE International Symposium on Mixed and Augmented Reality, ISMAR 2020, Recife/Porto de Galinhas, Brazil, November 9-13, 2020*. IEEE, 269–278. <https://doi.org/10.1109/ISMAR50242.2020.00050>
- [4] Joanna Bergström, Aske Mottelson, and Jarrod Knibbe. 2019. Resized grasping in vr: Estimating thresholds for object discrimination. In *Proceedings of the 32nd Annual ACM Symposium on User Interface Software and Technology*. 1175–1183. <https://doi.org/10.1145/3332165.3347939>
- [5] Eric Burns, Sharif Razzaque, Abigail Panter, Mary C. Whitton, Matthew R. McCalus, and Frederick P. Brooks. 2005. The hand is slower than the eye: a quantitative exploration of visual dominance over proprioception. *IEEE Proceedings. VR 2005. Virtual Reality, 2005.* (2005), 3–10.
- [6] Lung-Pan Cheng, Eyal Ofek, Christian Holz, Hrvoje Benko, and Andrew D Wilson. 2017. Sparse haptic proxy: Touch feedback in virtual environments using a general passive prop. In *Proceedings of the 2017 CHI Conference on Human Factors in Computing Systems*. 3718–3728.
- [7] Lung-Pan Cheng, Eyal Ofek, Christian Holz, Hrvoje Benko, and Andrew D. Wilson. 2017. Sparse Haptic Proxy: Touch Feedback in Virtual Environments Using a General Passive Prop. In *Proceedings of the 2017 CHI Conference on Human Factors in Computing Systems* (Denver, Colorado, USA) (CHI '17). Association for Computing Machinery, New York, NY, USA, 3718–3728. <https://doi.org/10.1145/3025453.3025753>
- [8] Inrak Choi, Yiwei Zhao, Eric J. Gonzalez, and Sean Follmer. 2021. Augmenting Perceived Softness of Haptic Proxy Objects Through Transient Vibration and Visuo-Haptic Illusion in Virtual Reality. *IEEE Trans. Vis. Comput. Graph.* 27, 12 (2021), 4387–4400. <https://doi.org/10.1109/TVCG.2020.3002245>
- [9] L. Dominjon, A. Lecuyer, J. Burkhardt, P. Richard, and S. Richir. 2005. Influence of control/display ratio on the perception of mass of manipulated objects in virtual environments. In *IEEE Proceedings. VR 2005. Virtual Reality, 2005.* 19–25. <https://doi.org/10.1109/VR.2005.1492749>
- [10] Marc O. Ernst and Martin S. Banks. 2002. Humans integrate visual and haptic information in a statistically optimal fashion. *Nature* 415, 6870 (Jan. 2002), 429–433. <https://doi.org/10.1038/415429a>
- [11] Marc O. Ernst and Heinrich H. Bühlhoff. 2004. Merging the senses into a robust percept. *Trends in Cognitive Sciences* 8, 4 (April 2004), 162–169. <https://doi.org/10.1016/j.tics.2004.02.002>
- [12] Shaghayegh Esmaeili, Brett Benda, and Eric D. Ragan. 2020. Detection of Scaled Hand Interactions in Virtual Reality: The Effects of Motion Direction and Task Complexity. In *IEEE Conference on Virtual Reality and 3D User Interfaces, VR 2020, Atlanta, GA, USA, March 22-26, 2020*. IEEE, 453–462. <https://doi.org/10.1109/VR46266.2020.158128532835>
- [13] Julian J. Faraway, Matthew P. Reed, and Jing Wang. 2007. Modelling three-dimensional trajectories by using Bézier curves with application to hand motion. *Journal of the Royal Statistical Society: Series C (Applied Statistics)* 56, 5 (2007), 571–585. <https://doi.org/10.1111/j.1467-9876.2007.00592.x> arXiv:<https://rss.onlinelibrary.wiley.com/doi/pdf/10.1111/j.1467-9876.2007.00592.x>
- [14] Benoît Geslain, Gilles Bailly, Sinan Haliyo, and Corentin Duboc. 2021. Visuo-haptic Illusions for Motor Skill Acquisition in Virtual Reality. In *Spatial User Interaction*. Virtual Venue, United States. <https://doi.org/10.1145/3485279.3485291>
- [15] James J Gibson. 1933. Adaptation, after-effect and contrast in the perception of curved lines. *Journal of experimental psychology* 16, 1 (1933), 1.
- [16] Eric J. Gonzalez, Parastoo Abtahi, and Sean Follmer. 2020. *REACH+: Extending the Reachability of Encountered-Type Haptics Devices through Dynamic Redirection in VR*. Association for Computing Machinery, New York, NY, USA, 236–248. <https://doi.org/10.1145/3379337.3415870>
- [17] Eric J Gonzalez and Sean Follmer. 2019. Investigating the Detection of Bimanual Haptic Retargeting in Virtual Reality. In *25th ACM Symposium on Virtual Reality Software and Technology*. 1–5.
- [18] Mar Gonzalez-Franco and Jaron Lanier. 2017. Model of illusions and virtual reality. *Frontiers in psychology* 8 (2017), 1125. <https://doi.org/10.3389/fpsyg.2017.01125>
- [19] Dustin T. Han, Mohamed Suhail, and Eric D. Ragan. 2018. Evaluating Remapped Physical Reach for Hand Interactions with Passive Haptics in Virtual Reality. *IEEE Transactions on Visualization and Computer Graphics* 24, 4 (2018), 1467–1476. <https://doi.org/10.1109/TVCG.2018.2794659>
- [20] D. A. G. Jauregui, F. Argelaguet, A. Olivier, M. Marchal, F. Multon, and A. Lecuyer. 2014. Toward "Pseudo-Haptic Avatars": Modifying the Visual Animation of Self-Avatar Can Simulate the Perception of Weight Lifting. *IEEE Transactions on Visualization and Computer Graphics* 20, 4 (April 2014), 654–661. <https://doi.org/10.1109/TVCG.2014.45>
- [21] L. Kohli. 2010. Redirected touching: Warping space to remap passive haptics. In *2010 IEEE Symposium on 3D User Interfaces (3DUI)*. 129–130. <https://doi.org/10.1109/3DUI.2010.5444703>
- [22] Luv Kohli, Eric Burns, Dorian Miller, and Henry Fuchs. 2005. Combining Passive Haptics with Redirected Walking. In *Proceedings of the 2005 International Conference on Augmented Tele-existence* (Christchurch, New Zealand) (ICAT '05). ACM, New York, NY, USA, 253–254. <https://doi.org/10.1145/1152399.1152451>
- [23] Przemyslaw A Lasota, Terrence Fong, Julie A Shah, et al. 2017. *A survey of methods for safe human-robot interaction*. Vol. 104. Now Publishers Delft, The Netherlands.
- [24] Flavien Lebrun, Sinan Haliyo, and Gilles Bailly. 2021. A Trajectory Model for Desktop-Scale Hand Redirection in Virtual Reality. In *IFIP Conference on Human-Computer Interaction*. Springer, 105–124.
- [25] Anatole Lécuyer, Sabine Coquillard, Abderrahmane Kheddar, Paul Richard, and Philippe Coiffet. 2000. Pseudo-haptic feedback: can isometric input devices simulate force feedback?. In *Proceedings IEEE Virtual Reality 2000 (Cat. No. 00CB37048)*. IEEE, 83–90.
- [26] Brandon J. Matthews, Bruce H. Thomas, G. Stewart Von Itzstein, and Ross T. Smith. 2019. Remapped Physical-Virtual Interfaces with Bimanual Haptic Retargeting. In *IEEE Conference on Virtual Reality and 3D User Interfaces, VR 2019, Osaka, Japan, March 23-27, 2019*. IEEE, 19–27. <https://doi.org/10.1109/VR.2019.8797974>
- [27] Nami Ogawa, Takuji Narumi, and Michitaka Hirose. 2021. Effect of Avatar Appearance on Detection Thresholds for Remapped Hand Movements. *IEEE Trans. Vis. Comput. Graph.* 27, 7 (2021), 3182–3197. <https://doi.org/10.1109/TVCG.2020.2964758>
- [28] Gonçalo Padrao, Mar Gonzalez-Franco, Maria V. Sanchez-Vives, Mel Slater, and Antoni Rodriguez-Fornells. 2016. Violating body movement semantics: Neural signatures of self-generated and external-generated errors. *NeuroImage* 124 (2016), 147 – 156. <https://doi.org/10.1016/j.neuroimage.2015.08.022>
- [29] Sharif Razzaque, Zachariah Kohn, and Mary C. Whitton. 2001. Redirected Walking. In *Eurographics 2001 - Short Presentations*. Eurographics Association. <https://doi.org/10.2312/egs.20011036>
- [30] Majed Samad, Elia Gatti, Anne Hermes, Hrvoje Benko, and Cesare Parise. 2019. Pseudo-Haptic Weight: Changing the Perceived Weight of Virtual Objects By Manipulating Control-Display Ratio. In *Proceedings of the 2019 CHI Conference on Human Factors in Computing Systems* (Glasgow, Scotland Uk) (CHI '19). ACM, New York, NY, USA, Article 320, 13 pages. <https://doi.org/10.1145/3290605.3300550>
- [31] Barry E Stein and M Alex Meredith. 1993. *The merging of the senses*. The MIT press.
- [32] Evan A Suma, Seth Clark, David Krum, Samantha Finkelstein, Mark Bolas, and Zachary Warte. 2011. Leveraging change blindness for redirection in virtual environments. In *2011 IEEE Virtual Reality Conference*. IEEE, 159–166. <https://doi.org/10.1109/VR.2011.5759455>
- [33] Qi Sun, Anjul Patney, Li-Yi Wei, Omer Shapira, Jingwan Lu, Paul Asente, Suwen Zhu, Morgan McGuire, David Luebke, and Arie Kaufman. 2018. Towards virtual reality infinite walking: dynamic saccadic redirection. *ACM Transactions on Graphics (TOG)* 37, 4 (2018), 1–13. <https://doi.org/10.1145/3197517.3201294>
- [34] Robert Sessions Woodworth. 1899. Accuracy of voluntary movement. *The Psychological Review: Monograph Supplements* 3, 3 (1899), i.
- [35] Andre Zenner and Antonio Krüger. 2019. Estimating Detection Thresholds for Desktop-Scale Hand Redirection in Virtual Reality. In *2019 IEEE Conference on Virtual Reality and 3D User Interfaces (VR)*. IEEE, 47–55.